J. Mech. Phys. Solids Vol. 40, No. 3, pp. 613–640, 1992.
Printed in Great Britain.

0022-5096/92 $5.00 + 0.00

STABILITY OF SOLIDS WITH INTERFACES

Z. SUO

Department of Mechanical Engineering, University of California at Santa Barbara, Santa Barbara, CA 93106, U.S.A.

and

M. ORTIZ† and A. NEEDLEMAN

Division of Engineering, Brown University, Providence, RI 02912, U.S.A.

(*Received* 7 *December* 1990; *in revised form* 2 *May* 1991)

ABSTRACT

STABILITY, in the sense of limits to the uniqueness of solutions to quasi-static boundary value problems, is investigated for two semi-infinite solids bonded along a planar interface. The interface is characterized by a traction–displacement jump relation, so that dimensional considerations introduce a characteristic length. Stability is addressed in terms of the existence of certain stationary waves. Complex variable methods are exploited to obtain an explicit solution when the interface instability precedes bulk localization. Particular cases are analyzed that illustrate a range of behaviors. Under certain conditions, a minimum wavelength for the instability mode is predicted that is at least one to two orders of magnitude larger than the interface constitutive characteristic length. A post-bifurcation analysis, carried out for linear elastic material behavior, shows how the instability plays a role in the transition from a uniform mode of separation to crack-like behavior. The results obtained suggest a mechanism for the size dependence of the failure mode.

1. INTRODUCTION

SEPARATION along interfaces plays a key role in limiting the ductility and toughness of a wide variety of solids. In certain circumstances, interfacial separation appears to involve the propagation of one or more initial crack-like defects along the bond line. In other circumstances, there is no clear evidence for initial defects, and, in principle, if the imposed loading were to permit it, decohesion could occur uniformly across the interface. In this paper a limit to the stability of such a uniform mode of decohesion is investigated.

Two solids, each occupying a half-space and bonded along a planar interface, are considered to be subject to remote loading that is consistent with their uniform separation. Each of the substrates is characterized as a time- and rate-independent solid. A constitutive relation of the type introduced in NEEDLEMAN (1987) is used to describe the response of the interface. This relation is also rate-independent and is

† Author to whom correspondence should be addressed.

expressed in terms of a relation between the displacement jump across the interface and the traction across the interface. For the issues addressed here, the precise form of the interfacial constitutive relation need not be specified. What is required is that, with increasing interfacial separation, the traction across the interface reaches a maximum and then decreases. Since the interfacial constitutive relation is expressed as a traction–displacement relation, dimensional considerations introduce a characteristic length.

Essentially, the interfacial stability issue investigated here is one of localization at an interface. As such, it is a question of the existence of certain stationary waves. In the limiting case of perfectly bonded substrates, the condition for interfacial stability corresponds to that for stationary Stoneley waves. In another limit, when the interface stiffness and that of one of the substrates vanishes, the condition reduces to one for stationary Rayleigh waves. In each of these cases, there is no characteristic length and, as is known from studies of surface and interface instabilities [e.g. HILL and HUTCHINSON (1975), HUTCHINSON and TVERGAARD (1980) and NEEDLEMAN and ORTIZ (1991)], arbitrarily short wavelength modes emerge. In the general case, because of the interface characteristic length, the interface waves are dispersive. Hence, the point at which the wavespeed vanishes depends on the wavelength. Furthermore, under certain circumstances, there is a minimum wavelength for the instability mode.

We begin by generalizing the stationary Stoneley wave analysis in NEEDLEMAN and ORTIZ (1991) to allow for a compliant interface. Quite general expressions for the conditions governing the onset of instability are obtained using a complex variable approach (STROH, 1958, 1962; SUO, 1990). Particular cases of orthotropic solids deforming in plane strain are analyzed to illustrate a range of behaviors. Finally, post-bifurcation results for the case of an elastic substrate on a rigid foundation are presented that show how the instability mode effects the transition from a uniform separation mode to propagation of a crack-like defect.

2. STATIONARY WAVES AT AN INTERFACE

We consider deformations that take the material point initially at $\mathbf{x}$ to $\bar{\mathbf{x}}$, where both $\mathbf{x}$ and $\bar{\mathbf{x}}$ are referred to a fixed Cartesian frame. The displacement vector $\mathbf{u}$ and the deformation gradient $\mathbf{F}$ are defined by

$$\mathbf{u} = \bar{\mathbf{x}} - \mathbf{x}, \quad \mathbf{F} = \frac{\partial \bar{\mathbf{x}}}{\partial \mathbf{x}}. \tag{2.1}$$

A Lagrangian formulation of the field equations is used with the current state taken as reference. Material points are identified by their Cartesian coordinates in the reference state. In terms of the unsymmetric nominal stress tensor, $\mathbf{s}$, which is related to the traction, $\mathbf{T}$, transmitted across a material element of area having orientation $\boldsymbol{\nu}$ in the reference configuration by $\mathbf{T} = \boldsymbol{\nu} \cdot \mathbf{s}$, the balance of linear momentum requires

$$s_{ij,i} = \rho \frac{\partial^2 u_j}{\partial t^2}, \tag{2.2}$$

where ρ is the mass density of the body in the reference configuration and $(\ )_{,i}$ denotes partial differentiation with respect to x_i. Writing (2.2) in rate form gives

$$\dot{s}_{ij,i} = \rho \frac{\partial^2 v_j}{\partial t^2}, \tag{2.3}$$

where ($\dot{}$) denotes differentiation with respect to time, and $v_j = \dot{u}_j$.

The material is modelled as rate-independent and the constitutive relation is expressed as

$$\dot{s}_{ij} = K_{ijkl}\dot{F}_{lk} = K_{ijkl}v_{l,k}. \tag{2.4}$$

The instantaneous stiffness tensor, **K**, may depend on the deformation history up to the current state, but it is taken to be independent of the current velocity.

As sketched in Fig. 1, two solids, each occupying a half-space and bonded along the plane $x_2 = 0$, are considered. Each half-space is presumed to be homogeneous in the current state and subject to incremental boundary conditions that are consistent with continuing homogeneous deformations. The response to small wave disturbances

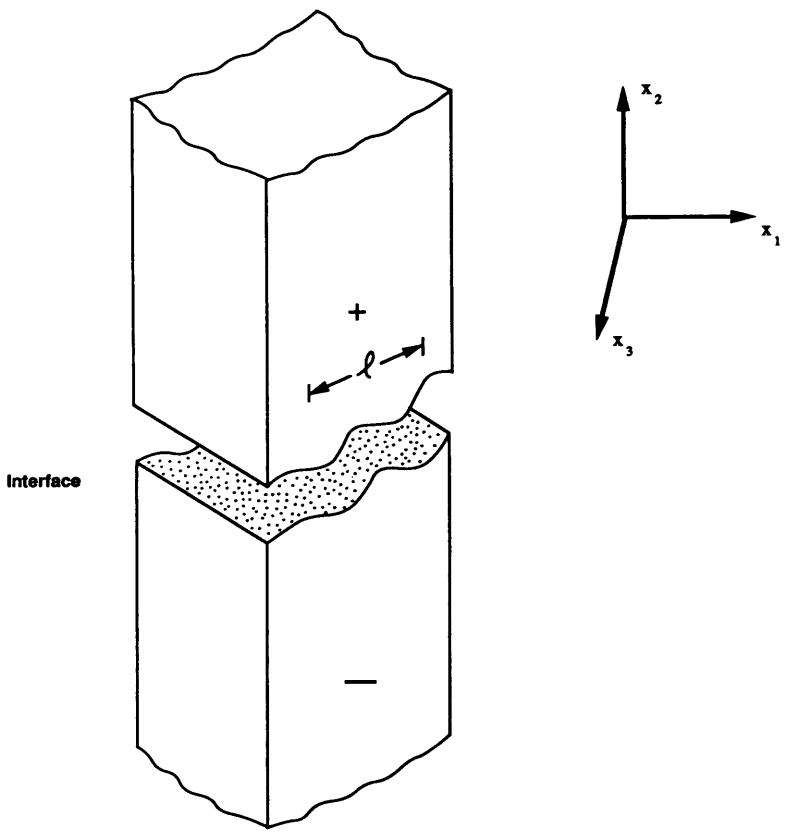

FIG. 1. Schematic illustrating two semi-infinite blocks bonded along a planar interface. An interface instability mode of orientation **k** is sketched.

about this state is investigated. Wave solutions that are periodic along the interface are sought. Hence, we write

$$v_j^+ = a_j^+ \exp[i(k_k^+ x_k - \kappa^+ ct)], \quad v_j^- = a_j^- \exp[i(k_k^- x_k - \kappa^- ct)], \tag{2.5}$$

where $(\,)^+$ and $(\,)^-$ denote the upper ($x_2 > 0$) and lower ($x_2 < 0$) sides of the interface, respectively, and $(\kappa^\pm)^2 = (k_1^\pm)^2 + (k_3^\pm)^2$. Because the velocity fields are periodic in the plane of the interface $k_1^\pm$ and $k_3^\pm$ are real.

The boundary conditions are that the traction rate is continuous across the interface and that this traction rate is related to the velocity jump across the interface by the interfacial constitutive relation. These boundary conditions can be written as

$$\dot{T}_j^+ + \dot{T}_j^- = 0, \quad \dot{T}_j^+ = -S_{jm}(v_m^+ - v_m^-) \quad \text{on} \quad x_2 = 0. \tag{2.6}$$

The instantaneous stiffness of the interface, **S**, is a 3 by 3 matrix of dimension [stress/length]. Specific examples of interfacial constitutive relations are given in NEEDLEMAN (1987, 1990), where the traction across the interface is derivable from a potential of the displacement jump. The instantaneous interface stiffness matrix **S** is then necessarily symmetric. More generally, the interface response can be path-dependent. Even with a path-dependent response, the instantaneous stiffness matrix may be symmetric, although there are circumstances, for example with frictional sliding along the interface, when **S** will necessarily be non-symmetric. For the present purposes, **S** may depend on the deformation jump history up to the current state, but is independent of the current velocity jump. Whatever the history dependence, the key feature of the interface response is that, with increasing separation, the traction across the interface reaches a maximum and then decreases. For a softening interface response, one or more eigenvalues of **S** are negative.

Since $v_2^\pm = \mp 1$ and $v_1^\pm = v_3^\pm = 0$, the traction rate boundary conditions become

$$\dot{T}_j^+ = -\dot{s}_{2j}^+, \quad \dot{T}_j^- = \dot{s}_{2j}^-. \tag{2.7}$$

Substituting (2.4) and (2.5) into the first of (2.6) gives

$$K_{2jkl}^- k_k^- a_l^- \exp[i(k_1^- x_1 + k_3^- x_3 - \kappa^- ct)] = K_{2jkl}^+ k_k^+ a_l^+ \exp[i(k_1^+ x_1 + k_3^+ x_3 - \kappa^+ ct)]. \tag{2.8}$$

From (2.8), traction rate continuity at each point of the interface requires $k_1^+ = k_1^- = k_1$, and $k_3^+ = k_3^- = k_3$.

For the velocity fields (2.5) to decay exponentially into the body, the conditions

$$\operatorname{Im} k_2^- \leqslant 0, \quad \operatorname{Im} k_2^+ \geqslant 0 \tag{2.9}$$

need to be satisfied. We now look for stationary wave solutions. Substituting (2.5) with $c = 0$ into (2.3) gives

$$a_l^+ k_k^+ k_i^+ K_{ijkl}^+ = 0, \quad a_l^- k_k^- k_i^- K_{ijkl}^- = 0, \tag{2.10}$$

which admit non-trivial solutions provided that

$$\det(k_k^+ k_i^+ K_{ijkl}^+) = 0, \quad \det(k_k^- k_i^- K_{ijkl}^-) = 0. \tag{2.11}$$

The quantities $k_2^\pm$ may be complex, due to the one-sided character of the solutions. In general, there will be six solutions of (2.11), say $k_2^{(\alpha)\pm}$ ($\alpha = 1$, 2 or 3). Let $a_j^{(\alpha)\pm}$

($\alpha = 1, 2$ or 3) be the corresponding amplitudes. Then, the general form of the solution with $c = 0$ is

$$v_j^{\pm} = \sum_{\alpha=1}^{3} a_j^{(\alpha)\pm} \exp\left[ik_k^{(\alpha)\pm} x_k\right]. \tag{2.12}$$

Furthermore, the amplitudes $a_j^{(\alpha)}$ must be consistent with (2.10). Let $q_l^{(\alpha)\pm}$ be the null eigenvector of the acoustic tensors $K_{ijkl}^{\pm} k_k^{(\alpha)\pm} k_i^{(\alpha)\pm}$. Then, the amplitude vectors must be of the form

$$a_j^{(\alpha)\pm} = a^{(\alpha)\pm} q_j^{(\alpha)\pm}. \tag{2.13}$$

Substituting (2.4), (2.2) and (2.13) into the boundary conditions (2.6) gives

$$\sum_{\alpha=1}^{3} S_{jm} q_m^{(\alpha)-} a^{(\alpha)-} - \sum_{\alpha=1}^{3} S_{jm} q_m^{(\alpha)+} a^{(\alpha)+} = \sum_{\alpha=1}^{3} [K_{2jkl}^{+} k_k^{(\alpha)+} q_l^{(\alpha)+}] a^{(\alpha)+},$$

$$\sum_{\alpha=1}^{3} [K_{2jkl}^{-} k_k^{(\alpha)-} q_l^{(\alpha)-}] a^{(\alpha)-} = \sum_{\alpha=1}^{3} [K_{2jkl}^{+} k_k^{(\alpha)+} q_l^{(\alpha)+}] a^{(\alpha)+}. \tag{2.14}$$

This is a system of six equations for the six unknowns $a^{(\alpha)\pm}$. The matrix of coefficients of this system is given by

$$M_{j\alpha} = S_{jm} q_m^{(\alpha)-}, \quad M_{(j+3)\alpha} = -S_{jm} q_m^{(\alpha)+} - K_{2jkl}^{+} k_k^{(\alpha)+} q_l^{(\alpha)+},$$

$$M_{j(\alpha+3)} = K_{2jkl}^{-} k_k^{(\alpha)-} q_l^{(\alpha)-}, \quad M_{(j+3)(\alpha+3)} = -K_{2jkl}^{+} k_k^{(\alpha)+} q_l^{(\alpha)+}. \tag{2.15}$$

For (2.15) to have non-trivial solutions, the matrix of coefficients must necessarily be singular, i.e.

$$\det(\mathbf{M}) = 0. \tag{2.16}$$

Several limiting cases are worth noting. First, when the compliance of the interface vanishes, i.e. when each $S_{mj}^{-1} = 0$, (2.14)–(2.16) reduce to the condition for stationary Stoneley waves in NEEDLEMAN and ORTIZ (1991). Next, if the $-$ substrate is rigid, then each $a^{(\alpha)-} = 0$ in the first of (2.14) and the second of (2.14) only serves to specify the traction rate along the rigid substrate. In this case, the boundary conditions give three equations for the three unknowns $a^{(\alpha)+}$ with the matrix of coefficients given by $M_{(m+3)\alpha}$ in (2.17). Finally, if both the $-$ substrate and the interface have zero stiffness, i.e. $\mathbf{K}^{-} = 0$ and $\mathbf{S} = 0$, each of (2.14) reduces to the traction-free condition for stationary Rayleigh waves.

3. ORTHOTROPIC SOLIDS ON RIGID SUBSTRATES

In this section, the effect of the interface response in promoting or retarding the onset of instability and on setting a characteristic wavelength is illustrated under plane strain conditions. The formulation takes a particularly simple form for the case of an incompressible solid, although incompressibility does necessitate a slight modification to the general framework. For an incompressible solid (2.3) and (2.4) become

$$\dot{s}_{ij,i} = \rho \frac{\partial^2 v_j}{\partial t^2} \tag{3.1}$$

and

$$\dot{s}_{ij} = K_{ijkl} v_{l,k} + \dot{p}\delta_{ij}. \tag{3.2}$$

For simplicity attention is restricted to a shear-free interface so that the only non-vanishing component of $\mathbf{S}$ is S_{22} and the deformable half-space is assumed subject to boundary conditions consistent with $\sigma_{12} = 0$ in the current state. Also, we confine attention to solids having instantaneous moduli that possess the symmetries $K_{ijkl} = K_{klij}$. Defining $\sigma_{11} = \sigma_1$ and $\sigma_{22} = \sigma_2$, the tensor of in-plane instantaneous moduli can be written in the form given by HILL and HUTCHINSON (1975), where

$$K_{1111} = \mu_* - \sigma_1, \quad K_{1122} = \mu_*, \quad K_{1112} = K_{1121} = 0, \tag{3.3}$$

$$K_{2211} = \mu_*, \quad K_{2222} = \mu_* - \sigma_2, \quad K_{2212} = K_{2221} = 0, \tag{3.4}$$

$$K_{1212} = \mu + \frac{\sigma}{2}, \quad K_{1221} = \mu - \sigma_m, \quad K_{2121} = \mu - \frac{\sigma}{2}, \tag{3.5}$$

with

$$\sigma_m = \tfrac{1}{2}(\sigma_1 + \sigma_2), \quad \sigma = (\sigma_2 - \sigma_1). \tag{3.6}$$

In plane-strain tension, the tangent modulus is $4\mu_*$ and μ is the instantaneous shear modulus.

The deformable solid is taken to lie in the half-space $x_2 \geqslant 0$ and for notational simplicity the superscript $+$ is dropped. Analogous to (2.12), we seek stationary wave solutions of the form

$$v_j = \sum_{\alpha=1}^{2} a_j^{(\alpha)} \exp\left[ik_k^{(\alpha)} x_k\right], \quad \dot{p} = i \sum_{\alpha=1}^{2} f^{(\alpha)} \exp\left[ik_k^{(\alpha)} x_k\right], \tag{3.7}$$

where $\alpha = 1$ or 2. Solutions are sought that are periodic in x_1, with wavelength $l = 2\pi/k_1$. Hence, k_1 is real and $k_1^{(1)} = k_1^{(2)} = k_1$. For convenience, we take $k_1 > 0$. Substituting (3.7) into the rate equilibrium equations (3.1) and using (3.2)–(3.6) gives

$$[p^{(\alpha)}]^4 \left(\mu + \frac{\sigma}{2}\right) + 2[p^{(\alpha)}]^2 (2\mu_* - \mu) + \left(\mu - \frac{\sigma}{2}\right) = 0, \tag{3.8}$$

where $p^{(\alpha)} = k_2^{(\alpha)}/k_1$.

The boundary conditions along $x_2 = 0$ are

$$(2\mu_* - \sigma_2) v_{2,2} + \dot{p} = -S_{22} v_2 \tag{3.9}$$

and

$$(\mu - \sigma_m) v_{2,1} + \left(\mu + \frac{\sigma}{2}\right) v_{1,2} = 0. \tag{3.10}$$

Substituting (3.7) into (3.9) and (3.10) gives

$$\begin{pmatrix} c_{11} & c_{12} \\ [ic_{21}+S_{22}/(k_1 p^{(1)})] & [ic_{22}+S_{22}/(k_1 p^{(2)})] \end{pmatrix} \begin{pmatrix} a_1^{(1)} \\ a_1^{(2)} \end{pmatrix} = 0, \tag{3.11}$$

where

$$c_{11} = \left(\mu+\frac{\sigma}{2}\right)[p^{(1)}]-(\mu-\sigma_m)\frac{1}{[p^{(1)}]}, \tag{3.12}$$

$$c_{12} = \left(\mu+\frac{\sigma}{2}\right)[p^{(2)}]-(\mu-\sigma_m)\frac{1}{[p^{(2)}]}, \tag{3.13}$$

$$c_{21} = -(\mu-\sigma_m)+\left(\mu-\frac{\sigma}{2}\right)\frac{1}{[p^{(1)}]^2}, \tag{3.14}$$

$$c_{22} = -(\mu-\sigma_m)+\left(\mu-\frac{\sigma}{2}\right)\frac{1}{[p^{(2)}]^2}. \tag{3.15}$$

Setting the determinant of coefficients in (3.11) to zero and using (3.8) gives

$$F+\frac{S_{22}}{k_1}G = 0, \tag{3.16}$$

where

$$F = (\mu-\sigma/2)(4\mu_*-2\sigma_m)+(\sigma_m^2-2\mu\sigma_m+\tfrac{1}{4}\sigma^2)p^{(1)}p^{(2)} \tag{3.17}$$

and

$$G = -(\mu+\sigma/2)\left[\frac{p^{(1)}+p^{(2)}}{i}\right]p^{(1)}p^{(2)}. \tag{3.18}$$

When the roots of (3.8) are complex, the two relevant roots are those for which $\mathrm{Im}\,[p^{(\alpha)}] > 0$. Then $p^{(1)}p^{(2)} < 0$ and (3.17) and (3.18) become

$$F = (\mu-\sigma/2)(4\mu_*-2\sigma_m)-(\sigma_m^2-2\mu\sigma_m+\tfrac{1}{4}\sigma^2)\sqrt{\frac{\mu-\sigma/2}{\mu+\sigma/2}} \tag{3.19}$$

and

$$G = (\mu+\sigma/2)\left[\frac{p^{(1)}+p^{(2)}}{i}\right]\sqrt{\frac{\mu-\sigma/2}{\mu+\sigma/2}}. \tag{3.20}$$

Since the interface stiffness has the dimension of stress/length, write $S_{22} = S/\delta$, where δ is an interfacial characteristic length. Then, using $k_1 = 2\pi/l$ ($l > 0$), (3.16) can be expressed as

$$F + \frac{Sl}{2\pi\delta} G = 0. \tag{3.21}$$

As a specific example of interface behavior, consider the exponential relation of ROSE *et al.* (1981, 1983),

$$T_2 = -\sigma_{\max} \frac{u_n}{\delta} \exp\left[-\left(\frac{u_n}{\delta} - 1\right)\right], \tag{3.22}$$

where $u_n = u_2(x_1, 0)$ is the interfacial separation and $\sigma_{\max}$ is the strength of the interface, which is attained at $u_n = \delta$. From (3.22)

$$S = \sigma_{\max}\left(1 - \frac{u_n}{\delta}\right)\exp\left[-\left(\frac{u_n}{\delta} - 1\right)\right]. \tag{3.23}$$

For a given stress state, μ_* and μ are known from the constitutive relation. Hence, F and G in (3.21) are known. From σ_2, the interfacial traction can be calculated as $T_2 = -\sigma_2/\lambda_2$, where λ_2 is the principal stretch along the x_2-direction and, because of incompressibility, $\lambda_1 = 1/\lambda_2$. Then, equilibrium and (3.22) determine the value of u_n. From (3.23), S is calculated. The relation (3.21) is an equation for the critical wavelength l.

Consider a deformation history corresponding to monotonically increasing σ_i and material behavior for which μ_* and μ are monotonically decreasing, and consider the possible solutions to (3.21). At small strains, μ_* and μ are presumed to be much larger than the $|\sigma_i|$ ($i = 1$ or 2). Also, assume that, at all stress levels, $\mu > |\sigma|/2$. Then, at small strains F and G are positive and (3.21) requires $u_n/\delta > 1$, so that instability requires the interface to be softening. Eventually $F = 0$, corresponding to stationary Rayleigh waves. In general at this point $G \neq 0$ and $S \neq 0$, so that (3.21) requires $l = 0$, a vanishingly short wavelength mode. As the stress level is increased, $F < 0$, and instability is possible with $u_n/\delta < 1$, so that the interface is hardening. A stress level is eventually reached for which (3.8) has real roots. This is the hyperbolic regime in which F is real and G is imaginary. Hence, in this regime a solution to (3.21) is possible only if either $S = 0$ or $l = 0$. There is, however, another possibility. In the hyperbolic regime all four roots of (3.8) satisfy (2.9) so that Im $[k_2] = 0$. Thus, as in NEEDLEMAN and ORTIZ (1991), there is the possibility of building up a solution from the corresponding four eigenfunctions. This will be illustrated within the context of the small-strain approximation.

3.1. *Small-strain approximations*

In the small-strain limit, the stress magnitudes are much smaller than either of the moduli, so that

$$\left|\frac{\sigma_i}{\mu}\right| \ll 1, \quad \left|\frac{\sigma_i}{\mu_*}\right| \ll 1, \quad i = 1, 2. \tag{3.24}$$

Throughout this section it will be assumed that $\mu > 0$. Given (3.24), the roots of (3.8) simplify to

$$[p^{(\alpha)}]^2 = \left(1-2\frac{\mu_*}{\mu}\right) \pm 2\frac{\mu_*}{\mu}\sqrt{1-\frac{\mu}{\mu_*}}. \tag{3.25}$$

From (3.19) and (3.20),

$$F \approx 4\mu\mu_*, \quad G \approx \mu\left[\frac{p^{(1)}+p^{(2)}}{i}\right]. \tag{3.26}$$

For an isotropic linear elastic solid $\mu = \mu_* = E/3$, where E is Young's modulus. Then,

$$p^{(1)} \approx i, \quad p^{(2)} \approx i. \tag{3.27}$$

Although $p^{(1)} = p^{(2)}$ in (3.27), the two roots do differ by terms of order σ/μ. Substituting (3.26) and (3.27) into (3.21) gives

$$\frac{4E}{3} + \frac{Sl}{\pi\delta} = 0. \tag{3.28}$$

Using (3.23) in (3.28) and solving for l gives

$$\frac{l}{\delta} = \frac{4E\pi \exp[-(1-u_n/\delta)]}{3\sigma_{\max}(u_n/\delta - 1)}. \tag{3.29}$$

Equation (3.29) expresses the bifurcation mode wavelength as a function of the interfacial separation u_n. Bifurcation into a long-wavelength mode, $l \to \infty$, first becomes possible (recall that the normalization adopted here requires $l > 0$) at $u_n = \delta$, i.e. when $S = 0$. Subsequently, bifurcation into shorter-wavelength modes can occur. However, with increasing u_n/δ, the critical wavelength increases again. The minimum bifurcation mode wavelength, $l_{\min}$, is found by setting the derivative of l with respect to u_n to zero. This gives

$$\frac{l_{\min}}{\delta} = \frac{4\pi eE}{3\sigma_{\max}} \approx 11.39\frac{E}{\sigma_{\max}}, \tag{3.30}$$

where $e = \exp[1]$.

The existence of a minimum wavelength is a consequence of the inflection point in the interface traction–separation relation (3.22). It is also worth noting that, for representative values of $E/\sigma_{\max}$, $l_{\min}$ is many times δ. For example, with $E/\sigma_{\max} = 50$, $l_{\min} \approx 569\delta$. Even for $E/\sigma_{\max} = 10$, which is representative of the theoretical strength of a homogeneous solid, $l_{\min} > 100\delta$.

From (3.7), with $k_2^{(\alpha)} = p^{(\alpha)}k_1$ and $k_1 = 2\pi/l$,

$$v_j = \sum_{\alpha=1}^{2} a_j^{(\alpha)} \exp[-x_2/D^{(\alpha)}] \exp[i(2\pi/l)(x_1 + \operatorname{Re} p^{(\alpha)} x_2)], \quad D^{(\alpha)} = \frac{l}{2\pi \operatorname{Im} p^{(\alpha)}}, \tag{3.31}$$

where $D^{(\alpha)}$ is the decay length and $\tan^{-1}[\operatorname{Re} p^{(\alpha)}]$ gives the orientation of the interface instability mode.

For small strains, with linear elastic material behavior, (3.27) implies that the decay length is $l/(2\pi)$ and the orientation is 0°.

Another limiting case of interest is when $\mu_*/\mu \ll 1$, with $\mu_* > 0$, while σ_i/μ_* terms are still negligible. This corresponds, for example, to the small-strain elastic–plastic solid. In this case,

$$p^{(1)} \approx 1+\sqrt{\frac{\mu_*}{\mu}}i, \quad p^{(2)} \approx -1+\sqrt{\frac{\mu_*}{\mu}}i, \tag{3.32}$$

so that the mode orientation is $\pm 45^\circ$ and the decay length is $[l/2\pi)]\sqrt{\mu/\mu_*}$. With μ fixed, the decay length increases with decreasing tangent stiffness μ_* and becomes unbounded for a non-hardening solid.

The analog to (3.28) is

$$4\sqrt{\mu_*\mu}+\frac{Sl}{\pi\delta}=0. \tag{3.33}$$

For a flow theory elastic–plastic solid with a smooth yield surface, we can write $\mu_* = E_t/3$ and $\mu = E/3$, where E_t, the tangent modulus, is the slope of the uniaxial true stress vs true strain curve. For a deformation theory solid, $\mu_* = E_t/3$ and $\mu = E_s/3$, where E_s is the secant modulus, i.e. true stress divided by true strain. The minimum wavelength is then given by

$$\frac{l_{\min}}{\delta}=\frac{4\pi e E_{\text{eff}}}{3\sigma_{\max}}, \tag{3.34}$$

where $E_{\text{eff}} = \sqrt{E_t E}$ for smooth yield surface flow theory and $E_{\text{eff}} = \sqrt{E_t E_s}$ for deformation theory. From (3.34), it can be seen that increased material compliance promotes a shorter minimum wavelength. However, as discussed in Section 3.2, strain reversal would generally occur before (3.33) is satisfied so that (3.34) is probably not relevant for elastic–plastic solids.

Now, we briefly consider circumstances where $\mu_* < 0$. Then with $|\mu_*/\mu| \equiv \beta \ll 1$, neglecting terms of order β but keeping terms of order $\sqrt{\beta}$, (3.25) gives

$$p^{(1)} \approx 1+\sqrt{\beta}, \quad p^{(2)} = -p^{(1)}, \quad p^{(3)} \approx -1+\sqrt{\beta}, \quad p^{(4)} = -p^{(3)}. \tag{3.35}$$

Here, since each $p^{(\alpha)}$ is real, the decay length is infinite and there are two sets of symmetric orientations.

Using all four eigenfunctions in (3.9) and (3.10) and neglecting terms of order stress divided by modulus gives

$$\sum_{\alpha=1}^{4}[p^{(\alpha)}-1/p^{(\alpha)}]a^{(\alpha)}=0 \tag{3.36}$$

and

$$\sum_{\alpha=1}^{4} i[-\mu+\mu/[p^{(\alpha)}]^2]a^{(\alpha)}+\frac{Sl}{2\pi\delta}\sum_{\alpha=1}^{4}[1/p^{(\alpha)}]=0. \tag{3.37}$$

Substituting (3.35) into (3.36) and (3.37) gives

$$a^{(1)} - a^{(2)} + a^{(3)} - a^{(4)} = 0 \tag{3.38}$$

and

$$-4i\mu\sqrt{\beta}[-a^{(1)} - a^{(2)} + a^{(3)} + a^{(4)}] + \frac{Sl}{2\pi\delta}\{(1-\sqrt{\beta})[a^{(1)} - a^{(2)}] + (-1+\sqrt{\beta})[a^{(3)} - a^{(4)}]\} = 0. \tag{3.39}$$

A solution to (3.38) and (3.39) for *any* S and *any* l is

$$a^{(1)} = a^{(2)}, \quad a^{(3)} = a^{(4)}, \quad a^{(1)} + a^{(2)} = a^{(3)} + a^{(4)}. \tag{3.40}$$

Solution (3.40) is available for all $\mu_*/\mu \leqslant 0$. For a non-hardening solid, $\mu_* = 0$ (it is assumed $\mu > 0$), the solutions $a^{(1)} = a^{(2)}$, $a^{(3)} = a^{(4)} = 0$ and $a^{(3)} = a^{(4)}$, $a^{(1)} = a^{(2)} = 0$ are also available. Within the small-strain approximation, $\mu_* = 0$ corresponds to the transition point at which the character of the governing equations shifts from elliptic to hyperbolic.

3.2. *Elastic solid at finite strain*

In order to illustrate finite strain behavior, consider a non-linear elastic solid for which the principal Cauchy stresses are related to the principal logarithmic strains by

$$\sigma_i = \frac{2E_s}{3}\varepsilon_i + p, \tag{3.41}$$

where $\varepsilon_i = \ln(\lambda_i)$, with the λ_i being the principal stretches, and E_s is the ratio of stress to strain on the uniaxial true stress–natural strain curve. This non-linear elastic constitutive relation has been used as a finite strain deformation theory of plasticity to explore a variety of tensile instability issues [e.g. HUTCHINSON and TVERGAARD (1980)].

In plane strain, with $\varepsilon_2 = -\varepsilon_1 = \varepsilon$, the traction T_2 is given by

$$T_2 = -\sigma_2 \exp(-\varepsilon). \tag{3.42}$$

The uniaxial stress–strain response is taken to follow the power law

$$\bar{\sigma} = K\bar{\varepsilon}^N, \tag{3.43}$$

where the Mises equivalent stress, $\bar{\sigma}$, and the Mises equivalent strain, $\bar{\varepsilon}$, are given in terms of the in-plane principal stress and strain components by

$$\bar{\sigma} = \frac{\sqrt{3}}{2}|\sigma_2 - \sigma_1|, \quad \bar{\varepsilon} = \frac{1}{\sqrt{3}}|\varepsilon_2 - \varepsilon_1|. \tag{3.44}$$

For this constitutive relation, the moduli μ_* and μ are given by

$$\mu_* = \frac{E_t}{3}, \quad \mu = \frac{E_s}{3}(\varepsilon_2 - \varepsilon_1)\coth(\varepsilon_2 - \varepsilon_1), \tag{3.45}$$

where $E_t = \mathrm{d}\bar{\sigma}/\mathrm{d}\bar{\varepsilon}$ and $E_s = \bar{\sigma}/\bar{\varepsilon}$.

Consider a deformation history that corresponds either to monotonically increasing interfacial separation or to monotonically increasing strain in the material. The stress ratio σ_1/σ_2 is taken to be fixed throughout the deformation history and the interface is described by (3.22). As will be seen shortly, in general, the interfacial separation and the material strain cannot both continue to increase monotonically.

Two possible situations are illustrated in Fig. 2. In Fig. 2(a), the maximum absolute value of T_2 in (3.42) is greater than $\sigma_{\max}$, while, in Fig. 2(b), it is less than $\sigma_{\max}$. First, consider the situation in Fig. 2(a). Both the interfacial separation and the material strain increase until the traction reaches $\sigma_{\max}$ and equilibrium prevents the traction in the material from exceeding this value. Hence, the decreasing traction with increasing interfacial separation means that the strain in the material decreases. In Fig. 2(b), when the maximum traction that the material can support is reached, the normal separation across the interface must decrease as the strain in the material increases. In this case, the interfacial response remains on the hardening branch. Thus, with continued loading either the material strain decreases or the interfacial separation decreases.

For fixed material properties, K and N, which of these two alternatives occurs depends on the stress ratio σ_1/σ_2. Figure 2(a) corresponds to a larger value of this ratio than does Fig. 2(b). To illustrate the implication for surface instability, take $K/\sigma_{\max} = 1.2$ and $N = 0.2$. The bifurcation behavior is determined in the following manner. For a given strain, ε, μ and μ_* can be calculated from (3.45). Since the ratio

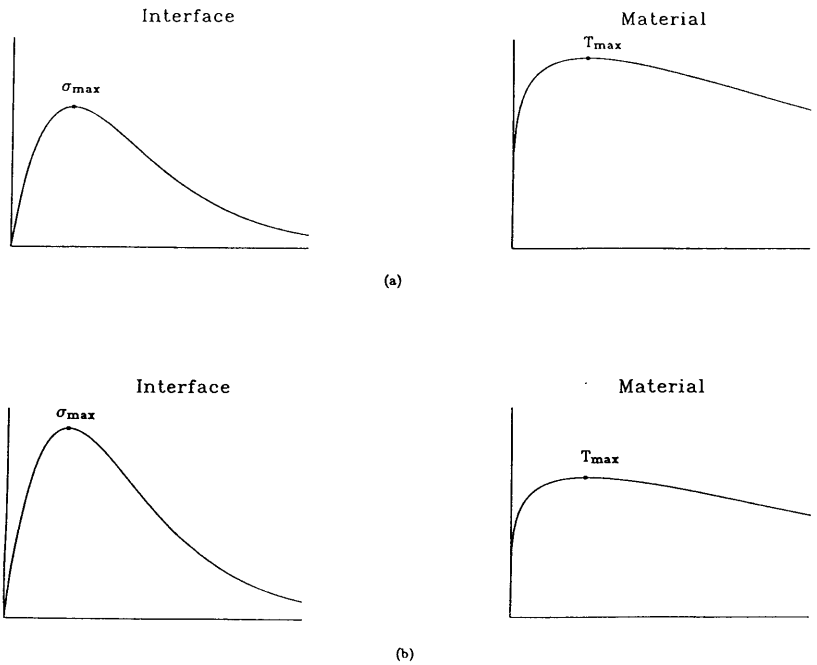

FIG. 2. (a) Interface traction–displacement jump relation and the material nominal load–strain relation with $\sigma_{\max} < T_{\max}$. (b) Interface traction–displacement jump relation and the material nominal load–strain relation with $\sigma_{\max} > T_{\max}$.

σ_1/σ_2 is specified and since $\bar{\sigma}$ is known as a function of ε, the stress state in the material is determined. The traction T_2 is known from equilibrium and (3.23) gives two values of S, one corresponding to softening and one to hardening, i.e. one with $u_n/\delta > 1$ and $S < 0$, and one with $u_n/\delta < 1$ and $S > 0$.

Figure 3 shows the bifurcation behavior for $\sigma_1/\sigma_2 = 0.2$. Figure 3(a) plots the value of $S/\sigma_{\max}$ as a function of strain, while Fig. 3(b) shows l/δ as a function of strain. Figure 3 corresponds to the behavior in Fig. 2(a) where the material undergoes strain rate reversal. For the parameter values of Fig. 3, the traction reaches $\sigma_{\max}$ when $\varepsilon = 0.09$. Decreasing strain in Fig. 3 corresponds to increasing interfacial separation. Bifurcation is possible at any point beyond the point at which the maximum traction is attained. However, near the maximum, the wavelength is very long as seen in Fig. 3(b). As separation increases, and strain in the material decreases, the bifurcation mode wavelength decreases. The minimum wavelength of 71.6δ is attained at $\varepsilon = 0.056$. At this point the decay length, $D^{(1)} = D^{(2)} = 27.1\delta$ and the orientations are $\pm 40.3^\circ$.

The values of K and N in Fig. 4 are the same as those used in Fig. 3, but here $\sigma_1/\sigma_2 = 0$. The behavior corresponds to that sketched in Fig. 2(b). The strain in the material increases monotonically and the interfacial separation decreases beyond the maximum traction point. Bifurcation first becomes possible when the condition $F = 0$ in (3.21) for stationary Rayleigh waves is reached. Since $S \neq 0$ and $G \neq 0$ at this point, $l = 0$. In Fig. 4(b), the critical wavelength increases with increasing strain.

In Fig. 3, where bifurcation takes place prior to the point at which stationary Rayleigh waves are possible, the interface length scale acts to set a minimum wavelength for the instability mode. On the other hand, in Fig. 4, the minimum wavelength is zero at the point where the stationary Rayleigh wave condition is satisfied. Thus, in this case the interface does not set a minimum wavelength.

As mentioned previously, this elastic constitutive relation has been used as a deformation theory of plasticity to investigate yield surface corner effects on plastic instability phenomena. The response of the elastic solid corresponds to that of the plastic solid as long as plastic loading continues. For the set of circumstances in Fig. 3, where strain reversal occurs in the material, bifurcation results for the non-linear elastic solid are not relevant for the plastic solid. Under strain reversal, the response of the plastic solid is governed by linear elastic moduli. Away from the point of strain reversal and away from any plastic reloading, the bifurcation analysis can be based on the linear elastic moduli. The minimum wavelength for the elastic unloading moduli is greater than for the less stiff loading moduli.

4. Formulation Based on Stroh's Representation

In the preceding sections attention is restricted to solutions having the exponential form (2.12). Consideration of that class of solutions suffices to determine local critical conditions for the onset of instability. An alternative approach which does not presuppose any *a priori* form of the solution uses Stroh's (1958, 1962) representation and the single complex variable methods of Suo (1990). For this complex variable formalism to apply, however, the equations are restricted to being elliptic. This is in

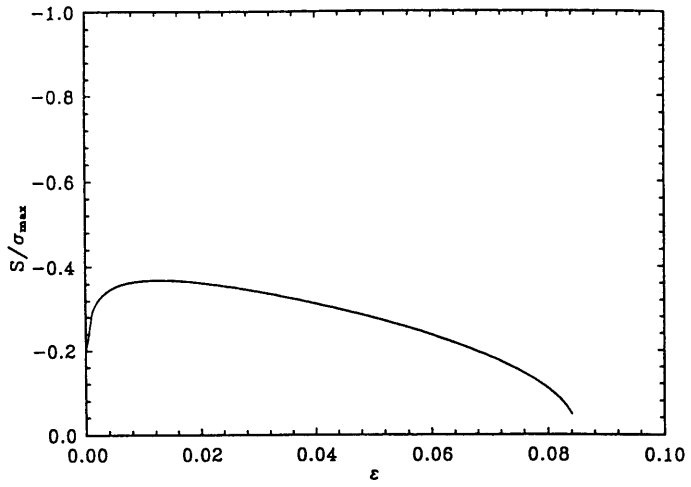

(a)

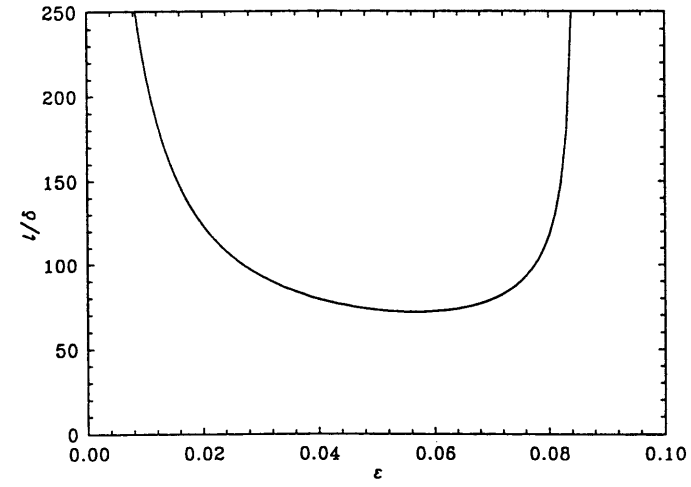

(b)

FIG. 3. Bifurcation behavior for a case where $\sigma_{max} < T_{max}$ as in Fig. 2(a): $K/\sigma_{max} = 1.2$ and $N = 0.2$ in (3.43), and $\sigma_1/\sigma_2 = 0.2$. (a) Interface stiffness for bifurcation, S/σ_{max}, vs strain, ε. (b) Instability wavelength, l, normalized by the interface characteristic length, δ, vs strain, ε. In both (a) and (b) decreasing strains correspond to increasing separation.

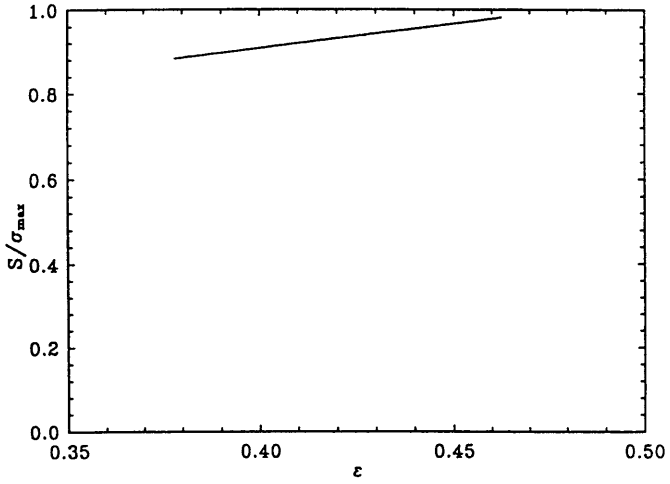

(a)

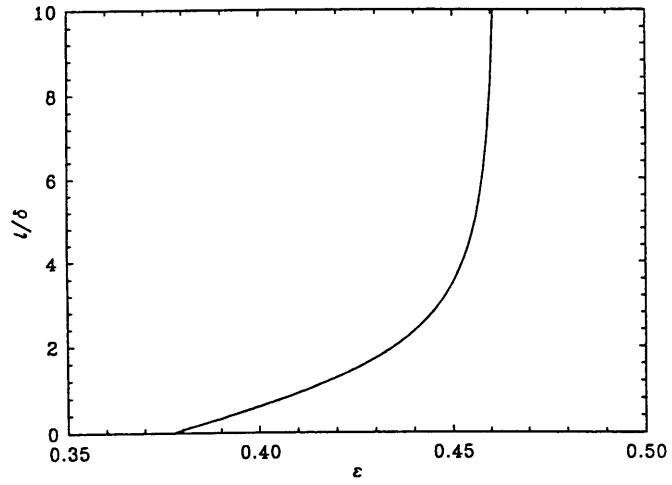

(b)

FIG. 4. Bifurcation behavior for a case where $\sigma_{max} > T_{max}$ as in Fig. 2(b); $K/\sigma_{max} = 1.2$ and $N = 0.2$ in (3.43), and $\sigma_1/\sigma_2 = 0$. (a) Interface stiffness for bifurcation, S/σ_{max}, vs strain, ε. (b) Instability wavelength, l, normalized by the interface characteristic length, δ, vs strain, ε.

contrast to the formulation in Section 2, which applies regardless of the type of the equations and can therefore be used to investigate the effect of the interface on localization in the solid. This limitation notwithstanding, the complex variable formulation is useful in deriving explicit results in certain cases, as demonstrated in Section 5.

Substituting (2.4) into (2.3) gives

$$(K_{ijkl}v_{l,k})_{,i} = \rho\frac{\partial^2 v_j}{\partial t^2}. \tag{4.1}$$

Consider a homogeneously deformed homogeneous solid, so that K_{ijkl} is independent of $\mathbf{x}$, and seek superposed incremental wave solutions having wavespeed c along the x_1-direction. Define the coordinates

$$x = x_1 - ct, \quad y = x_2. \tag{4.2}$$

In terms of the stationary wave analysis given in the preceding sections, x is identified with the direction of the interface wave, i.e. x measures distance in the plane of the interface along the direction specified by (k_1, k_3), while $y = x_2$ measures distance normal to the interface which lies on the plane $y = 0$. Attention here is restricted to stationary wave solutions for which $c \equiv 0$. Then, the in-plane momentum balance equations take the form

$$K_{ijkl}v_{l,ki} = 0, \quad i,k = 1,2, \quad j,l = 1,2,3. \tag{4.3}$$

The tensor of moduli $\mathbf{K}$ is assumed to possess the symmetry

$$K_{ijkl} = K_{klij}. \tag{4.4}$$

Furthermore, it is assumed that the moduli satisfy the ellipticity condition

$$a_i b_j K_{ijki} a_k b_l > 0 \tag{4.5}$$

for arbitrary vectors $\mathbf{a}$ and $\mathbf{b}$ for which $\|\mathbf{a}\| > 0$ and $\|\mathbf{b}\| > 0$.

Attention is further restricted to two-dimensional, non-homogeneous velocity fields of the form

$$v_k = v_k(x, y), \quad k = 1,2,3. \tag{4.6}$$

Substituting (4.6) into (4.3) defines a set of constant coefficient second-order linear partial differential equations, whose general solution is given by an arbitrary function of a linear combination of x and y,

$$\mathbf{v} = \mathbf{a}f(x+py). \tag{4.7}$$

The vector $\mathbf{a}$ and scalar p are determined by substituting (4.7) into (4.3), which gives

$$[\mathbf{Q}+p(\mathbf{R}+\mathbf{R}^T)+p^2\mathbf{T}]\mathbf{a} = 0, \tag{4.8}$$

where

$$Q_{jl} = K_{1j1l}, \quad R_{jl} = K_{1j2l}, \quad T_{jl} = K_{2j2l}. \tag{4.9}$$

The assumed symmetry of the moduli, (4.4), requires $\mathbf{Q}$ and $\mathbf{T}$ to be symmetric

matrices, but places no restrictions on **R**. By recourse to the ellipticity condition (4.4), ESHELBY *et al.* (1953) showed that the eigenvalue problem (4.8) determines three pairs of complex conjugate roots. Let $p^{(1)}$, $p^{(2)}$ and $p^{(3)}$ be the roots with positive imaginary parts. The velocity field can be represented as a linear combination of three arbitrary functions f_1, f_2 and f_3 of the form

$$\mathbf{v} = 2\,\mathrm{Re}\sum_{\alpha=1}^{3}\mathbf{a}^{(\alpha)}f_\alpha[x+p^{(\alpha)}y], \tag{4.10}$$

where $\mathbf{a}^{(\alpha)}$ is the eigenvector associated with $p^{(\alpha)}$. Let $z^{(\alpha)} = x+p^{(\alpha)}y$, and denote

$$\mathbf{A} = [\mathbf{a}^{(1)}, \mathbf{a}^{(2)}, \mathbf{a}^{(3)}], \quad \mathbf{P} = \mathrm{diag}\,[p^{(1)}, p^{(2)}, p^{(3)}]. \tag{4.11}$$

Once the potentials $f_1[z^{(1)}]$, $f_2[z^{(2)}]$ and $f_3[z^{(3)}]$ are found for a particular boundary value problem, the velocities v_i and stress rates $\dot{s}_{ij}$ follow as

$$\begin{aligned} v_i &= 2\,\mathrm{Re}\sum_{\alpha=1}^{3}A_{i\alpha}f_\alpha[z^{(\alpha)}], \\ \dot{s}_{2i} &= 2\,\mathrm{Re}\sum_{\alpha=1}^{3}L_{i\alpha}f'_\alpha[z^{(\alpha)}], \\ \dot{s}_{1i} &= -2\,\mathrm{Re}\sum_{\alpha=1}^{3}L_{i\alpha}p^{(\alpha)}f'_\alpha[z^{(\alpha)}], \end{aligned} \tag{4.12}$$

where $(\,)'$ denotes differentiation with respect to the argument. The matrix **L** is derived from (4.2) and (4.10) with the result

$$\mathbf{L} = \mathbf{R}^T\mathbf{A}+\mathbf{T}\mathbf{A}\mathbf{P}. \tag{4.13}$$

Assuming that the roots $p^{(1)}$, $p^{(2)}$ and $p^{(3)}$ are distinct, STROH (1958) showed that **A** and **L** are non-singular matrices. Further, the matrix **B**, defined as

$$\mathbf{B} = i\mathbf{A}\mathbf{L}^{-1}, \tag{4.14}$$

is a positive-definite Hermitian matrix, provided that the moduli possess the symmetry (4.4) [see BARNETT and LOTHE (1985) for more properties of this compliance-like matrix, and the implications for Rayleigh and Stoneley waves]. Note that $\mathbf{B} = \mathbf{Z}^{-1}$, where **Z** is the impedance tensor in their article.

The above complex variable representation is essentially identical to the one developed by LEKHNITSKII (1981), ESHELBY *et al.* (1953) and STROH (1958) for elastic solids, although, unlike the small-strain theories considered by those authors, here the moduli need not possess minor symmetries. Following SUO (1990), we consider vector functions of $z = x+\zeta y$ ($\mathrm{Im}\,\zeta > 0$) of the form

$$\mathbf{f}(z) = \{f_1(z), f_2(z), f_3(z)\}. \tag{4.15}$$

Note the arguments for the three component functions are identical. Solutions to particular boundary value problems can be given in terms of functions of this type. For given $\mathbf{f}(z)$, the velocity and stress rate fields are computed from (4.12) using f_1, f_2 and f_3 with arguments $z^{(1)}$, $z^{(2)}$ and $z^{(3)}$, respectively. This approach, as demonstrated subsequently, allows standard algebraic operations to be combined with concepts of

analytic functions of *one* variable. Of particular importance are the velocity and traction rate along the x-axis:

$$\mathbf{v}(x) = \{v_i(x,0)\} = \mathbf{A}\mathbf{f}(x) + \bar{\mathbf{A}}\bar{\mathbf{f}}(x),$$
$$\dot{\mathbf{t}}(x) = \{\dot{s}_{2j}(x,0)\} = \mathbf{L}\mathbf{f}'(x) + \bar{\mathbf{L}}\bar{\mathbf{f}}'(x), \tag{4.16}$$

implied by (4.12) and (4.15).

Now consider two semi-infinite solids bonded at an interface. The solid is presumed to be homogeneously deformed up to current state. To accommodate any difference in lateral contraction, different values of s_{1j} may be required on the two sides of the interface. From (4.16), traction continuity is satisfied if

$$\mathbf{L}^+\mathbf{f}^+(x) + \bar{\mathbf{L}}^+\bar{\mathbf{f}}^+(x) = \mathbf{L}^-\mathbf{f}^-(x) + \bar{\mathbf{L}}^-\bar{\mathbf{f}}^-(x) \tag{4.17}$$

holds along the entire interface $y = 0$, $-\infty < x < \infty$. The above equation can be rearranged to read

$$\mathbf{L}^+\mathbf{f}^+(x) - \bar{\mathbf{L}}^-\bar{\mathbf{f}}^-(x) = \mathbf{L}^-\mathbf{f}^-(x) - \bar{\mathbf{L}}^+\bar{\mathbf{f}}^+(x). \tag{4.18}$$

In this relation, the left-hand side corresponds to a function which is analytic in the upper half-plane, while the right-hand side is analytic in the lower half-plane. Hence, both sides can be analytically continued into the entire plane. Since both sides vanish at infinity, they must be zero for any $z = x + \zeta y$ (Im $\zeta > 0$). Thus it follows that

$$\mathbf{L}^+\mathbf{f}^+(z) = \bar{\mathbf{L}}^-\bar{\mathbf{f}}^-(z) = \mathbf{g}(z) \quad (y > 0) \tag{4.19}$$

for some function $\mathbf{g}(z)$ analytic in $y > 0$. Making use of (4.16), the traction rate and velocities at the interface can now be expressed in terms of $\mathbf{g}(x)$ as

$$\dot{\mathbf{t}}(x) = \mathbf{g}'(x) + \bar{\mathbf{g}}'(x) \tag{4.20}$$

and

$$\mathbf{v}^+(x) = -i\mathbf{B}^+\mathbf{g}(x) + i\bar{\mathbf{B}}^+\bar{\mathbf{g}}(x),$$
$$\mathbf{v}^-(x) = -i\mathbf{B}^-\bar{\mathbf{g}}(x) + i\bar{\mathbf{B}}^-\mathbf{g}(x). \tag{4.21}$$

Inserting (4.20) and (4.21) into the incremental interface constitutive relation (2.6) results in the relation

$$\mathbf{g}'(x) + \bar{\mathbf{g}}'(x) = -i\mathbf{S}[\mathbf{H}\mathbf{g}(x) - \bar{\mathbf{H}}\bar{\mathbf{g}}(x)], \tag{4.22}$$

where one defines

$$\mathbf{H} = \mathbf{B}^+ + \bar{\mathbf{B}}^-. \tag{4.23}$$

We note that if $\mathbf{B}^{\pm}$ are both positive-definite Hermitian matrices, so is $\mathbf{H}$. Analytic continuation considerations applied to (4.22) yield

$$\mathbf{g}'(z) = -i\mathbf{S}\mathbf{H}\mathbf{g}(z). \tag{4.24}$$

This is an ordinary differential equation with constant coefficients, the solution of which takes the form

$$\mathbf{g}(z) = \mathbf{q}\exp(2\pi iz/l). \tag{4.25}$$

The vector $\mathbf{q}$ and scalar l are determined by direct substitution of (4.25) into (4.24), which yields the generalized eigenvalue problem

$$\mathbf{SHq} = -\frac{2\pi}{l}\mathbf{q}. \tag{4.26}$$

Assume now that $\mathbf{S}$ is symmetric. Since, additionally, $\mathbf{H}$ is Hermitian, it follows that all three eigenvalues of (4.28) are real. The limit of an infinitely stiff interface, $\mathbf{S}^{-1} \to \mathbf{0}$, gives rise to $l \to 0$, while $l \to \infty$ as the interface stiffness vanishes, i.e. $\mathbf{S} \to \mathbf{0}$.

To ensure that $\mathbf{g}$ vanishes as $y \to +\infty$, the roots l must be positive. When $\mathbf{H}$ is positive-definite, a positive eigenvalue l exists iff $\mathbf{S}$ is *not* positive-definite, i.e. iff $\mathbf{S}$ is negative-definite or indefinite. Conversely, if $\mathbf{H}$ is negative-definite, a positive eigenvalue l exists iff $\mathbf{S}$ is positive-definite or indefinite. These correspond to the situations in Fig. 3 and Fig. 4, respectively.

For a given positive-definite root l and the associated eigenvector $\mathbf{q}$, the vector potentials in the two constituent solids are given by

$$\begin{aligned}\mathbf{L}^{+}\mathbf{f}^{+}(z) &= \mathbf{q}\exp(2\pi iz/l) \quad (y > 0),\\ \mathbf{L}^{-}\mathbf{f}^{-}(z) &= \bar{\mathbf{q}}\exp(-2\pi iz/l) \quad (y < 0).\end{aligned} \tag{4.27}$$

The velocity and stress fields follow by inserting (4.27) into the representation (4.12). For simplicity, we give the field quantities in the upper solid only, with the superscript + dropped. Denote

$$\mathbf{Y} = \operatorname{diag}\{\exp[2\pi ip^{(1)}y/l], \quad \exp[2\pi ip^{(2)}y/l], \quad \exp[2\pi ip^{(3)}y/l]\}. \tag{4.28}$$

Then

$$\begin{aligned}\mathbf{v}(x, y) &= 2\,\mathrm{Re}[\exp(2\pi ix/l)\mathbf{AYL}^{-1}\mathbf{q}],\\ \{\dot{s}_{2i}(x, y)\} &= -\frac{4\pi}{l}\,\mathrm{Im}[\exp(2\pi ix/l)\mathbf{LYL}^{-1}\mathbf{q}],\\ \{\dot{s}_{1i}(x, y)\} &= \frac{4\pi}{l}\,\mathrm{Im}[\exp(2\pi ix/l)\mathbf{LYPL}^{-1}\mathbf{q}].\end{aligned} \tag{4.29}$$

Evidently, the fields are periodic in x with wavelength l. In addition, the fields decay exponentially with y with decay lengths

$$D^{(\alpha)} = \frac{l}{2\pi\,\mathrm{Im}[p^{(\alpha)}]} \quad \alpha = 1, 2, 3. \tag{4.30}$$

As in the stationary wave treatment, the role of the interface in introducing a definite length scale into the solution is noteworthy. In the limiting case in which $\mathbf{S}^{-1} \to \mathbf{0}$, it follows from (4.26) that $l \to 0$, and, consequently, the decay lengths (4.30) themselves vanish. This limit corresponds to two dissimilar solids constrained to satisfy velocity compatibility across the interface, in which case the problem lacks an intrinsic length scale, and the decay lengths scale with the wavelength of the solution.

5. AN INTERFACE BETWEEN IDENTICAL ORTHOTROPIC SOLIDS

We specialize the general results derived in the preceding section to the case of two identical semi-infinite solids bonded at an interface. The solid is assumed to remain orthotropic throughout the history of deformation, with the principal axes of orthotropy coincident with x and y. Assume further that the current stresses are negligibly small relative to the instantaneous moduli of the solid, so that, in addition to (4.4), $K_{ijkl} = K_{jikl} = K_{ijlk}$. We shall restrict attention to plane-strain deformations. The instantaneous compliances b_{ij} are defined such that

$$\begin{pmatrix} v_{1,1} \\ v_{2,2} \\ v_{1,2}+v_{2,1} \end{pmatrix} = \begin{bmatrix} b_{11} & b_{12} & 0 \\ b_{21} & b_{22} & 0 \\ 0 & 0 & b_{66} \end{bmatrix} \begin{pmatrix} \dot{s}_{11} \\ \dot{s}_{22} \\ \dot{s}_{12} \end{pmatrix}. \tag{5.1}$$

Following SUO (1990), we introduce the dimensionless parameters

$$\lambda = \frac{b_{11}}{b_{22}}, \quad \rho = \frac{2b_{12}+b_{66}}{2(b_{11}b_{22})^{1/2}} \tag{5.2}$$

which measure the degree of in-plane orthotropy: $\lambda = \rho = 1$ for isotropic solids, and $\lambda = 1$ for solids with cubic symmetry. The ellipticity condition (4.5) requires that

$$\lambda > 0, \quad \rho > -1. \tag{5.3}$$

The characteristic equation (4.8) specializes to

$$\lambda p^4 + 2\rho\lambda^{1/2}p^2 + 1 = 0. \tag{5.4}$$

The roots with positive imaginary parts are

$$p^{(1)}, p^{(2)} = \begin{cases} i\lambda^{-1/4}(n+m), & i\lambda^{-1/4}(n-m), & \text{for } 1 < \rho < \infty \\ \lambda^{-1/4}(in+m), & \lambda^{-1/4}(in-m), & \text{for } -1 < \rho < 1 \\ i\lambda^{-1/4}, & i\lambda^{-1/4}, & \text{for } \rho = 1, \end{cases} \tag{5.5}$$

where $n = [(1+\rho)/2]^{1/2}$ and $m = |(1-\rho)/2|^{1/2}$. The degenerate case $\rho = 1$ will not be treated here explicitly. The two fundamental matrices arising in the complex variable formulation are

$$\mathbf{L} = \begin{bmatrix} -p^{(1)} & -p^{(2)} \\ 1 & 1 \end{bmatrix}, \quad \mathbf{A} = \begin{bmatrix} b_{11}[p^{(1)}]^2 + b_{12} & b_{11}[p^{(2)}]^2 + b_{12} \\ b_{21}p^{(1)} + b_{22}/p^{(1)} & b_{21}p^{(2)} + b_{22}/p^{(2)} \end{bmatrix}. \tag{5.6}$$

The matrix $\mathbf{H}$ is given by

$$\mathbf{H} = 4n(b_{11}b_{22})^{1/2} \begin{bmatrix} \lambda^{1/4} & 0 \\ 0 & \lambda^{-1/4} \end{bmatrix} \tag{5.7}$$

and the eigenvalues of (4.26) are

$$l_1 = -\frac{\pi}{n\sqrt{b_{11}b_{22}}}[\lambda^{1/4}S_{11}+\lambda^{-1/4}S_{22}+\sqrt{(\lambda^{1/4}S_{11}-\lambda^{-1/4}S_{22})^2+4S_{12}S_{21}}]^{-1},$$

$$l_2 = -\frac{\pi}{n\sqrt{b_{11}b_{22}}}[\lambda^{1/4}S_{11}+\lambda^{-1/4}S_{22}-\sqrt{(\lambda^{1/4}S_{11}-\lambda^{-1/4}S_{22})^2+4S_{12}S_{21}}]^{-1}. \quad (5.8)$$

Because ellipticity of the constituent solids is assumed from the outset, the possible range of behavior described by the above solutions is somewhat more limited than that uncovered by the stationary wave analysis given in Sections 2 and 3. For purposes of illustration, envision, for example, a process of deformation in the solid such that the interface undergoes uniform and monotonic separation and sliding, resulting in steadily decreasing values of S_{11} and S_{22}. Both S_{11} and S_{22} are assumed to be initially positive, with l_1 and l_2 negative, so that no solution exists other than the uniform solution. A bifurcation first becomes possible when either l_1 or l_2 change sign. This happens when the product $l_1 l_2$ vanishes, which, from (5.8), requires

$$S_{11}S_{22}-S_{12}S_{21} = 0. \quad (5.9)$$

In the exceptional case in which separation and sliding are uncoupled, $S_{12} = 0$ and the bifurcation condition (5.9) requires that either S_{11} or S_{22} be zero. This in turn implies that either the separation or the sliding response, or both, must become non-hardening. More generally, if $S_{12} \neq 0$ and $S_{12}S_{21} > 0$, which is certainly the case if $S_{12} = S_{21}$, then bifurcation can occur while both $S_{11} > 0$ and $S_{22} > 0$. Thus we reach the conclusion that coupling between separation and sliding generally promotes interfacial instability.

The earliest possible instabilities have infinite wavelength and infinite decay length. If bifurcation can be delayed beyond the maximum cohesive traction, then instabilities with finite wavelength and decay length are possible. The wavelength of the unstable mode may or may not have a minimum depending on details of the interface constitutive relation. Consider, for instance, the limiting case of an isotropic solid and let $S_{12} = 0$. Assume that the pre-bifurcation stress state is one of plane-strain tension and that the interface undergoes separation only. Put $S_{22} = -S/\delta$, for some interfacial characteristic length δ, and $l_2 = l$. Then (5.8b) reduces to

$$l = \frac{\pi E'}{S}\delta, \quad (5.10)$$

where E' is the plane-strain Young's modulus, $E' = E/(1-\nu^2)$, with E being Young's modulus and ν Poisson's ratio. Hence, l attains a minimum $l_{\min}$ iff S attains a maximum, say $S_{\max}$, and

$$l_{\min} = \frac{\pi E'}{S_{\max}}\delta. \quad (5.11)$$

This in turn requires the interface constitutive relation to have an inflection point in its softening branch. From the relation of Rose *et al.* (1981, 1983), (3.23), with u_n the full separation between the + and − half-spaces, (5.11) gives

$$l_{\min} = \frac{e\pi E'}{\sigma_{\max}}\delta \approx 8.54\frac{E'}{\sigma_{\max}}\delta. \tag{5.12}$$

With $\nu = \frac{1}{2}$, $l_{\min}$ as given by (5.12) is the same as the corresponding value (3.30) for an elastic solid on a rigid substrate in plane strain. As pointed out in Section 3, the values of $l_{\min}$ predicted by (3.30) and, hence, (5.12) are at least two orders of magnitude larger than δ for representative values of E and $\sigma_{\max}$.

6. POST-BIFURCATION BEHAVIOR

The preceding analyses have been concerned with the determination of critical conditions for bifurcation. By their nature, the analyses convey no information about the behavior of the interface following bifurcation, i.e. about the post-bifurcation regime. In some simple cases, however, it is possible to characterize the post-bifurcation regime to some extent. The following example falls into this category.

Consider a semi-infinite solid occupying the region $y > 0$, and assume that the solid is bonded to a rigid substrate along the plane $y = 0$. The solid is linear elastic and is subject to a remote tensile stress σ_∞ normal to the interface. The interface obeys a constitutive law of the form

$$\sigma(u) = 4\sigma_{\max}\left[\frac{u}{\delta} - \left(\frac{u}{\delta}\right)^2\right], \quad u \leqslant \delta$$

$$\sigma(u) = 0, \quad u \geqslant \delta, \tag{6.1}$$

where, since geometry changes are neglected, σ is the traction on the interface, and u the separation at the bond line, which for a rigid substrate coincides with the normal displacement at the boundary. The interfacial traction is initially a quadratic function of the separation, vanishes at a critical separation δ, and is identically zero beyond that point (Fig. 5).

Assume additionally that the solid undergoes plane-strain deformations in the x–y plane. Then, the normal displacement on the boundary of the solid is governed by a

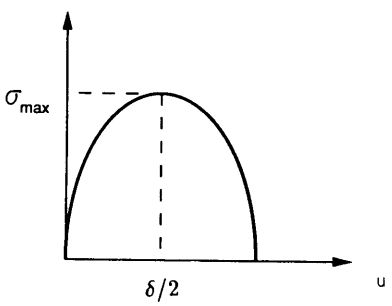

FIG. 5. Interface traction–displacement jump relation specified by (6.1).

standard integral equation of linear elasticity (MUSKHELISHVILI, 1953), which, suitably specialized to the present conditions, reads

$$\frac{\mu}{2\pi(1-\nu)}\int_{-\infty}^{\infty}\frac{u'(\xi)\,d\xi}{x-\xi}+\sigma[u(x)]=\sigma_\infty, \tag{6.2}$$

where μ is the shear modulus. Equation (6.2) always admits the trivial solution $u(x)=A$, which corresponds to a uniform separation. It is readily verified by direct substitution that the expression

$$u(x)=A+\frac{B}{1+(x/a)^2} \tag{6.3}$$

defines a family of solutions of (6.2), with the coefficients given by

$$A=\frac{\delta}{2}-\frac{B}{4},$$

$$B=2\delta\sqrt{1-\frac{\sigma_\infty}{\sigma_{\max}}},$$

$$a=\frac{E'}{8\sigma_{\max}}\frac{\delta}{\sqrt{1-\sigma_\infty/\sigma_{\max}}}, \tag{6.4}$$

where $E'=E/(1-\nu^2)$. By translation invariance, any function of the type $u(x+c)$, for arbitrary c, is likewise a solution.

The family of solutions defined above corresponds to a hump-like opening profile [Fig. 6(a)]. Solutions of this type exist only if $\sigma_\infty \leqslant \sigma_{\max}$, which ensures that B and a are real. The width of the hump is measured by the length parameter a. When $\sigma_\infty=\sigma_{\max}$, the width a of the opening profile is infinite. For $\sigma_\infty<\sigma_{\max}$, the opening displacements within a certain interval about the origin lie on the decreasing part of the interface traction–displacement relation, $u(x)>\delta$, while those in the complementary region lie on the increasing part, $u(x)<\delta$. The maximum separation occurs at $x=0$, and takes the value $u_{\max}=A+B$. For $u_{\max}>\delta$, a fully decohered region with vanishing stresses spreads out from the origin, and solution (6.3) is no longer valid. The condition $u_{\max}=\delta$, which determines the range of validity of (6.3), gives

$$\sigma_\infty=\frac{8\sigma_{\max}}{9}, \tag{6.5}$$

at which point

$$a=\frac{3E'}{8\sigma_{\max}}\delta. \tag{6.6}$$

The full range of behavior of the interface can now be characterized, at least conceptually. Imagine that a solid with a perfectly flat interface is loaded by a rigid device which prescribes the maximum opening displacement $u(x=0)=u_{\max}$. Initially, for $u_{\max}<\delta/2$, the separation at the interface is uniform, which corresponds to taking $B=0$ in (6.3). During this range, $\sigma(x)<\sigma_{\max}$ everywhere. The point of instability

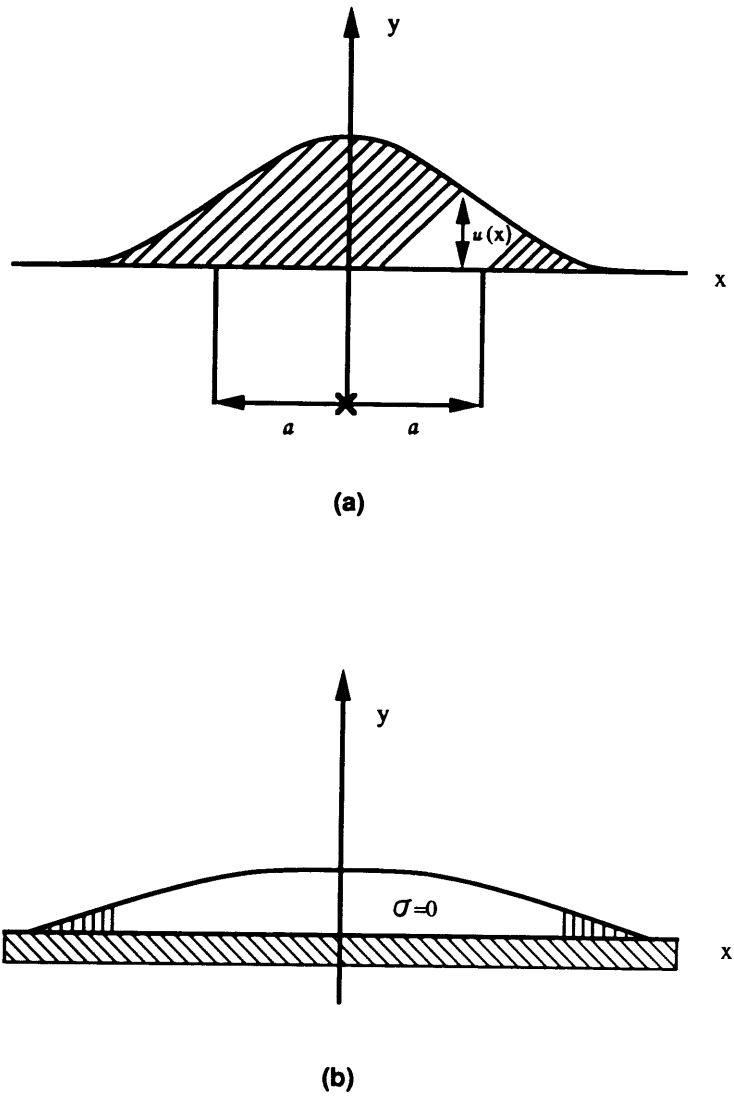

FIG. 6. (a) Opening profile in the post-bifurcation regime. (b) Interface crack with a cohesive zone.

occurs at $u_{max} = \delta/2$, i.e. at the maximum attainable stress $\sigma_\infty = \sigma_{max}$, in agreement with the bifurcation analyses given in the preceding sections. At bifurcation, $a = \infty$, i.e. the width of the hump is infinite. Further separation takes place with decreasing applied stress. Thus, in this range, $\sigma_\infty < \sigma_{max}$. The separation ceases to be uniform, and is given by (6.3). As the maximum separation increases, the applied stress drops to the value (6.5), at which point the cohesive stress vanishes at the origin. Subsequently, a

fully decohered zone in which the cohesive stresses vanish spreads out from the origin, and solution (6.3) ceases to be valid.

At some point, the fully decohered zone becomes much larger than the characteristic width of the cohesive zones, and begins to behave as a Dugdale–Barenblatt crack (DUGDALE, 1960; BARENBLATT, 1962), as sketched in Fig. 6(b). The cohesive zones lie deep within the square-root singular fields at the tips of the crack. A standard application of the J-integral of RICE (1968) then shows that the apparent critical energy release rate for the growth of the crack equals the work of separation of the interface, i.e. the area under the interface traction–displacement jump relation. For the simple model defined in (6.1), the critical energy release rate is readily computed to be

$$\mathcal{G}_c = \tfrac{2}{3}\sigma_{\max}\delta. \tag{6.7}$$

Since here the stress intensity factor increases with increasing crack length, a critical stress intensity factor criterion implies that the crack continues to grow under decreasing applied stress.

From this perspective, it is evident that the solution (6.3) represents the early stages of a transition from uniform separation to crack-like interfacial separation. The debonding of the interface takes place in three stages. First, uniform separation occurs, followed by a bifurcation into a localized decohesion mode. The terminal stage of debonding is crack-like.

7. Summary and Discussion

The analysis given in this paper extends earlier work by NEEDLEMAN and ORTIZ (1991) to the case of two semi-infinite solids bonded along a planar interface which can separate and slide according to an interface constitutive relation. The aim here is to characterize the range of stability, understood as uniqueness of the solution, of the bimaterial–interface system. The onset of instability is identified with the point at which stationary waves first become possible. The significance of stationary waves stems from their role in signalling the transition from stability to instability; when all possible wavespeeds c are such that $c^2 > 0$, then there is stability with respect to small disturbances; when $c^2 < 0$ for some waves, there is divergence-type growth, as noted by RICE (1977). For instance, the emergence of stationary body waves signals the onset of bulk localization (HADAMARD, 1903; HILL, 1962; MANDEL, 1966; RICE, 1977), whereas the existence of stationary Rayleigh waves, or failure of the complementing condition, characterizes the loss of stability at free boundaries. NEEDLEMAN and ORTIZ (1991) have adopted the criterion of the existence of stationary Stoneley waves to investigate the stability of perfectly bonded interfaces.

In the present context, the waves of interest may be termed 'interfacial waves', and represent wave-like relative motions of the interface. Rayleigh and Stoneley waves are limiting cases corresponding to infinitely "soft" and "stiff" interfaces, respectively. As emphasized by NEEDLEMAN and ORTIZ (1991), in addition to defining the stability limit, such stationary wave solutions are amenable to a shear band interpretation and, therefore, furnish information concerning the local orientation and decay lengths of the emerging shear bands. In the circumstances considered here, such stationary

interfacial waves determine the orientation and decay lengths of shear bands crossing an interface. A special feature which stems from the interface constitutive law, and which is not present in the Rayleigh and Stoneley wave cases, is an intrinsic length scale that can set a scale for the instability mode wavelength and decay length.

In some notable cases, the analysis predicts a minimum wavelength for the instability. Interestingly, the minimum wavelength is typically orders of magnitude larger than the characteristic length of the interface. For instance, in coherent interfaces between elastic crystals, where the interfacial length scale is of the order of the atomic spacing, the minimum wavelength predicted by the analysis is roughly two orders of magnitude larger. Conveniently, this lends *a posteriori* validity to the continuum treatment of the solid bordering on the interfaces, by virtue of the fact that all deformations of interest vary over length scales much larger than the atomic spacing.

As illustrated by the results of NEEDLEMAN and ORTIZ (1991), stability may be lost by localization within the constituent solids while the interface remains stable, in the sense that stationary body waves become possible within one or both of the constituent solids before the condition for the existence of interfacial waves is satisfied. In this case, the interface acts as a barrier to localization. Under other circumstances, stability may be lost at the interface first, in the sense that stationary interfacial waves become possible while stationary body waves are precluded. In this case, the interface acts to promote instability. The stability of the interface itself, i.e. the question of existence of stationary interfacial waves, depends critically on details of the constitutive response of the solid and of the interface.

For example, in the simple plane-strain tension problem considered in Section 3, if the strength of the interface is less than the maximum support load of the solid, the interfacial response dominates and the interface characteristic length sets the minimum instability wavelength. On the other hand, if the strength of the interface is greater than the maximum support load of the solid, the material response dominates and, since the material constitutive relations considered here have no intrinsic length scale, vanishingly small wavelength instabilities are possible.

An appealing aspect of the complex variable approach of STROH (1958, 1962) and SUO (1990) is that the form of the solution is not presupposed beforehand, but is determined from the particular boundary value problem under consideration. However, applicability of the method requires the problem to be elliptic. This restriction ensures that the roots of the characteristic polynomial are complex conjugate, so that two-dimensional solutions can be expressed in terms of analytic functions of a complex variable. The analyticity of certain functions and their decay properties at infinity are invoked explicitly in deriving the general solution, which is sought in a form uniformly valid over the entire complex plane. When ellipticity is lost, some of the characteristic roots become real and the complex variable treatment of the problem breaks down. By way of contrast, the analysis in Section 2 is, in essence, a local analysis and is thus not restricted by the type of the equations.

The complex variable formulation yields alternative expressions for the unstable modes and permits their explicit computation in certain cases. A configuration which has been treated in some detail concerns two identical semi-infinite solids bonded at a planar interface. These results reveal some insights into the process of formation of new surfaces in the interior of a solid. For instance, we have found that, when

separation and sliding are coupled and the cohesive law derives from a potential, an interfacial instability can occur below the cohesive strength of the solid. If, by contrast, as in Section 3 here, one assumes that pure sliding does not affect the separation response, instability first becomes possible at the cohesive strength of the interface.

Finally, we have been able to characterize the initial post-bifurcation response in the simple case of an elastic solid separating from a rigid substrate according to a parabolic cohesive law. The separation profile exhibits a single central hump and steadily decays to zero at infinity. Solutions of this type exist only beyond the cohesive strength, and thus correspond to the post-bifurcation regime. The width of the opening profile is initially infinite, consistent with the bifurcation analysis, and decreases thereafter. At some point, a fully decohered zone in which the cohesive stresses vanish spreads out from the center of the instability. Eventually, the fully decohered zone becomes much larger than the characteristic width of the cohesive zones, and the solid begins to exhibit crack-like behavior. From this perspective, the present results suggest a size-dependent transition from a more or less uniform mode of interfacial separation to fracture.

Consider an interface that has a finite extent in the direction specified by the wave vector **k** and circumstances where localization at the interface occurs before a material instability in the bulk and where the load carrying capacity of the bulk material is greater than the strength of the interface. If appropriate boundary conditions are imposed along the sides orthogonal to **k**, then the modes obtained here are possible instability modes. If the finite extent of the body is smaller than the minimum instability wavelength (which is much larger than the interface characteristic length), separation can occur more or less uniformly. If this extent is larger than the minimum wavelength, instability can occur and failure would be by crack nucleation and growth. This interface contact length can be identified with the length of a grain boundary facet in a polycrystalline solid or with a reinforcing particle edge length in a composite material.

Other crack nucleation mechanisms are of course possible and may occur before the instability mode considered here, for example crack nucleation due to the stress concentration at grain boundary triple points. Another crack nucleation mechanism that merits investigation occurs when localization in the bulk precedes localization at the interface. The stress and strain concentrations that are induced when the bulk shear band meets the interface could nucleate a crack. In such a case, as indicated by the analysis in Section 3, the interface characteristic length does not set a size scale. In order to set a size scale, e.g. for shear band widths, some other characteristic length needs to be incorporated into the analysis.

Acknowledgements

ZS gratefully acknowledges support from a National Science Foundation research initiation award (MSS-9011571) and from ONR/URI contract N00014-86-K-0753. MO and AN are grateful for the support provided by the Brown University Materials Research Group on the Micromechanics of Failure Resistant Materials, funded by the National Science Foundation.

References

Barenblatt, G. I. 1962 *Adv. appl. Mech.* **7**, 56.
Barnett, D. M. and Lothe, J. 1985 *Proc. R. Soc.* **A402**, 135.

DUGDALE, D. S. 1960 *J. Mech. Phys. Solids* **8,** 100.
ESHELBY, J. D., READ, W. T. and SHOCKLEY, W. 1953 *Acta Metall.* **1,** 251.
HADAMARD, J. 1903 *Leçons sur la Propagation des Ondes et les Équations de l'Hydrodynamique*, Chap. 6. Librairie Scientifique A. Herrmann, Paris. (Also 1949. Chelsea, New York.)
HILL, R. 1962 *J. Mech. Phys. Solids* **10,** 1.
HILL, R. and HUTCHINSON, J. W. 1975 *J. Mech. Phys. Solids* **23,** 239.
HUTCHINSON, J. W. and TVERGAARD, V. 1980 *Int. J. mech. Sci.* **22,** 339.
LEKHNITSKII, S. G. 1981 *Theory of Elasticity of an Anisotropic Body*. Mir, Moscow.
MANDEL, J. 1966 In *Rheology and Soil Mechanics* (edited by J. KRAVTCHENKO and P. M. SIRIEYS), p. 58. Springer, Berlin.
MUSKHELISHVILI, N. I. 1953 *Singular Integral Equations*. Noordhoff, Leyden.
NEEDLEMAN, A. 1987 *J. appl. Mech.* **54,** 525.
NEEDLEMAN, A. 1990 *J. Mech. Phys. Solids* **38,** 289.
NEEDLEMAN, A. and ORTIZ, M. 1991 *Int. J. Solids Struct.* **28,** 859.
RICE, J. R. 1968 *J. appl. Mech.* **35,** 379.
RICE, J. R. 1977 IN *Theoretical and Applied Mechanics* (edited by W. T. KOITER). North-Holland, Amsterdam.
ROSE, J. H., FERRANTE, J. and SMITH, J. R. 1981 *Phys. Rev. Lett.* **47,** 675.
ROSE, J. H., SMITH, J. R. and FERRANTE, J. 1983 *Phys. Rev.* **B28,** 1835.
STROH, A. N. 1958 *Phil. Mag.* **7,** 625.
STROH, A. N. 1962 *J. Math. Phys.* **41,** 77.
SUO, Z. 1990 *Proc. R. Soc.* **A427,** 331.